

8463

NACA TN 2036

# NATIONAL ADVISORY COMMITTEE FOR AERONAUTICS

TECHNICAL NOTE 2036

CHARTS OF AIRPLANE ACCELERATION RATIO  
FOR GUSTS OF ARBITRARY SHAPE

By Bernard Mazelsky

Langley Aeronautical Laboratory  
Langley Air Force Base, Va.



Washington  
February 1950

AFMDC  
TECHNICAL LIBRARY  
AFL 2811

0065367



TECH LIBRARY KAFB, NM



## NATIONAL ADVISORY COMMITTEE FOR AERONAUTICS

## TECHNICAL NOTE 2036

## CHARTS OF AIRPLANE ACCELERATION RATIO

## FOR GUSTS OF ARBITRARY SHAPE

By Bernard Mazelsky

## SUMMARY

The equation of vertical motion for an airplane flying in gusty air is simplified in order that its solution is a function of only two parameters, namely, the mass parameter of the airplane and the shape of the gust the airplane is penetrating. The solutions of the equation are presented in the form of charts that can be used for estimating rapidly and easily the acceleration ratios encountered by airplanes with different mass parameters penetrating a sharp-edge gust, a gust of arbitrary shape, or a triangular gust.

## INTRODUCTION

For many problems of gust loads it has been found practical to calculate the loads as if they were for a rigid airplane restrained in pitch under the action of the gust. Although previous investigations have presented solutions for particular mass parameters and gust shapes, they have not been found sufficiently accurate. In the present paper the equation of motion has therefore been solved for a large range of mass parameters to obtain charts of airplane reactions to specific gusts and to provide a means for obtaining loads on airplane wings for arbitrary gust shapes. The charts presented are based on two-dimensional unsteady-lift curves and a numerical solution of the equation of motion.

## SYMBOLS

$\frac{dC_L}{d\alpha}$	slope of wing lift curve, per radian
$\rho$	mass density of air, slugs per cubic foot
$V$	forward velocity, feet per second

$W$	airplane weight, pounds
$S$	area of wing, square feet
$c$	mean aerodynamic chord, feet
$g$	acceleration due to gravity, feet per second per second
$s$	penetration into gust, chords
$\Delta s$	increment of $s$ used in numerical solution
$C_{L_g}$	normalized unsteady-lift function due to penetration of a sharp-edge gust
$F_m$	forcing function in recurrence formula due to penetration of gust
$C_{L_\alpha}$	normalized unsteady-lift function for a unit change of angle of attack
$A_m$	transformed unsteady-lift function $(1 - C_{L_\alpha}(s))$
$U$	gust velocity, feet per second
$H, H_1, H_2, \dots$	gradient distances of gusts, chords
$\mu_g$	mass parameter $\left( \frac{2W}{\rho \frac{dC_{L_g}}{d\alpha} Scg} \right)$
$\Delta n(s)$	load-factor increment
$\Delta n_g$	load-factor increment as computed by the gust-load formula $\left( \frac{\rho \frac{dC_{L_{VSU_{max}}}}{d\alpha}}{2W} \right)$
$\Delta n(s)/\Delta n_g$	acceleration ratio

$\left(\frac{\Delta n(s)}{\Delta n_s}\right)_{seg}$	acceleration ratio for penetration of a sharp-edge gust
I	integral of acceleration ratio $\Delta n/\Delta n_s$
Subscripts:	
max	maximum value
m	integer denoting m increments of s in recurrence formula (s/ $\Delta s$ )
1	denotes point at which solution applies

#### DERIVATION AND USE OF CHARTS

The following assumptions are made for stating the equation of motion:

(1) The gust velocity is uniform across the span and parallel to the vertical axis of the airplane at any instant.

(2) The airplane is in steady level flight prior to entry into the gust.

(3) The airplane can rise but does not pitch under the action of the gust.

(4) The airplane is rigid.

(5) The lift increment of the horizontal tail due to the gust and the airplane motions is negligible as compared to the wing lift increment.

The following equation for describing the vertical motion of the airplane is written in terms of acceleration ratios:

$$\frac{\Delta n(s_1)}{\Delta n_s} = \int_0^{s_1} C_{L_g}(s_1 - s) \frac{d\left(\frac{U(s)}{U_{max}}\right)}{ds} ds - \frac{1}{\mu_g} \int_0^{s_1} C_{L_\alpha}(s_1 - s) \frac{\Delta n(s)}{\Delta n_s} ds \quad (1)$$

The first term on the right represents the force due to the gust and the second, the alleviation due to the vertical motion of the airplane.

The values of the load-factor increment  $\Delta n_g$  and mass parameter  $\mu_g$  may be obtained from the characteristics of the airplane and its flight conditions by the following equations:

$$\Delta n_g = \frac{\rho \frac{dC_{L_{VSU}}}{d\alpha}_{\max}}{2W} \quad (2)$$

and

$$\mu_g = \frac{2W}{\rho \frac{dC_{L_{Scg}}}{d\alpha}} \quad (3)$$

#### Sharp-Edge Gust

For a sharp-edge gust (fig. 1(a)), equation (1) can be rewritten

$$\left( \frac{\Delta n(s_1)}{\Delta n_g} \right)_{\text{seg}} = C_{L_g}(s) - \frac{1}{\mu_g} \int_0^{s_1} C_{L_\alpha}(s_1 - s) \frac{\Delta n(s)}{\Delta n_g} ds \quad (4)$$

Equation (4) has been solved by a numerical method according to reference 1 and the solution is written in the form of a recurrence formula. Utilizing the procedure in this reference and making substitutions for the unsteady-lift functions gives the numerical solution of equation (4) in recurrence form; thus,

$$\begin{aligned} \left( \frac{\Delta n}{\Delta n_g} \right)_m &= K_1 F_m + K_2 I_{m-1} + K_3 \left( \frac{\Delta n}{\Delta n_g} \right)_{m-1} + K_4 \left( \frac{\Delta n}{\Delta n_g} \right)_{m-2} + K_5 \left( \frac{\Delta n}{\Delta n_g} \right)_{m-3} \\ &+ K_6 \left( \frac{\Delta n}{\Delta n_g} \right)_{m-4} + K_7 \left( \frac{\Delta n}{\Delta n_g} \right)_{m-5} + K_8 \left( \frac{\Delta n}{\Delta n_g} \right)_{m-6} \end{aligned} \quad (5)$$

where

$$F_m = C_{L_g}(m) = C_{L_g}(s)$$

$$I_m = I_{m-1} + \frac{\Delta s}{24} \left[ 9 \left( \frac{\Delta n}{\Delta n_s} \right)_m + 19 \left( \frac{\Delta n}{\Delta n_s} \right)_{m-1} - 5 \left( \frac{\Delta n}{\Delta n_s} \right)_{m-2} + \left( \frac{\Delta n}{\Delta n_s} \right)_{m-3} \right] \quad (6)$$

$$K_1 = \frac{1}{\left[ 1 + \frac{\Delta s}{\mu_g} \left( \frac{9}{24} - \frac{A_0}{3} \right) \right]} \quad (7a)$$

$$K_2 = -\frac{1}{\mu_g} K_1 \quad (7b)$$

$$K_3 = \frac{K_1 \Delta s}{\mu_g} \left( \frac{4A_1}{3} - \frac{19}{24} \right) \quad (7c)$$

$$K_4 = \frac{K_1 \Delta s}{\mu_g} \left( \frac{5}{24} + \frac{2A_2}{3} \right) \quad (7d)$$

$$K_5 = \frac{K_1 \Delta s}{\mu_g} \left( \frac{4A_3}{3} - \frac{1}{24} \right) \quad (7e)$$

$$K_6 = \frac{2 \Delta s K_1 A_4}{3 \mu_g} \quad (7f)$$

$$K_7 = \frac{4 \Delta s K_1 A_5}{3 \mu_g} \quad (7g)$$

$$K_8 = \frac{\Delta s K_1 A_6}{3 \mu_g} \quad (7h)$$

and

$$A_m = 1 - C_{L\alpha}(s) \quad (8)$$

Equation (5) is evaluated for a range of mass parameters from 10 to 100 and the results are shown in figure 2. In the calculations, the unsteady-lift functions derived for the two-dimensional wing are assumed to be made applicable to the finite wing by replacing the slope of the lift curve for the two-dimensional wing by the slope of the lift curve for the finite wing. These unsteady-lift functions due to penetration of a sharp-edge gust  $C_{Lg}(s)$  and an instantaneous unit angle-of-attack change  $C_{L\alpha}(s)$  for a two-dimensional wing were normalized from those given in reference 2.

Although equation (4) can be solved in closed form by means of operators, the solution is unwieldy and the numerical method was adopted for ease in computation.

The inaccuracies incurred in the solution by the numerical method are principally a function of the mass parameter  $\mu_g$  and the increment  $\Delta s$ . For high values of  $\mu_g$  and small values of  $\Delta s$  the accuracy of the calculation is increased, conversely for low values of  $\mu_g$  and large values of  $\Delta s$  the accuracy is decreased. When the recurrence equation was evaluated, the value of  $\Delta s$  was appropriately changed for the range of  $\mu_g$  considered.

## Arbitrary Gust Shape

In order to calculate the response to an arbitrary gust shape, the response to a sharp-edge gust may be used as an indicial response with the gust shape as a forcing function in Duhamel's integral. (See reference 3.) Thus,

$$\frac{\Delta n(s_1)}{\Delta n_s} = \int_0^{s_1} \left( \frac{\Delta n}{\Delta n_s} \right)_{\text{seg}} (s_1 - s) \frac{d \left( \frac{U(s)}{U_{\text{max}}} \right)}{ds} ds \quad (9)$$

Various methods are given in reference 4 for evaluating equation (9) numerically; however, if the forcing function consists of a series of straight lines, equation (9) can be modified by the following procedure: For a linear disturbance starting from  $s = 0$  with a slope  $1/H$  and extending to infinity (fig. 1(b)), equation (9) can be rewritten as follows:

$$\frac{\Delta n(s)}{\Delta n_s} = \frac{1}{H} \int_0^s \left( \frac{\Delta n(s)}{\Delta n_s} \right)_{\text{seg}} ds \quad (10)$$

This equation can be evaluated for different mass parameters by merely integrating the function  $\left( \frac{\Delta n(s)}{\Delta n_s} \right)_{\text{seg}}$  for different values of mass parameter and multiplying the result by the constant  $1/H$ . In figure 3 the integrations of the  $\left( \frac{\Delta n(s)}{\Delta n_s} \right)_{\text{seg}}$  responses are given for a range of mass parameters. When the ordinates for a curve are multiplied by the slope  $1/H$ , the resulting response is the solution of equation (10). By superposition of a series of functions of the type given by equation (10), this approach may be extended to predict the responses to disturbances of the type shown in figure 1(c) where the disturbance is composed of straight-line segments. Figure 3 is used to evaluate this response by the following steps:



(a) Evaluate the following integrals in a manner similar to that used for equation (10), with the aid of figure 3:

$$\left. \begin{aligned} \frac{1}{H_1} I(s) \\ \frac{1}{H_2} I(s) \\ \frac{1}{H_3} I(s) \\ \frac{1}{H_4} I(s) \end{aligned} \right\} \quad (11)$$

(b) Superpose the time histories obtained from step (a) so that the disturbance function shown in figure 1(c) will be formed by the addition of the slopes  $1/H_1$ ,  $1/H_2$ ,  $1/H_3$ , and  $1/H_4$ . Note that in the course of this superposition, the functions corresponding to the slopes  $1/H_2$ ,  $1/H_3$ , and  $1/H_4$  must be displaced by the intervals  $H_1$  for the slope  $1/H_2$ ,  $H_1 + H_2$  for the slope  $1/H_3$ , and  $H_1 + H_2 + H_3$  for the slope  $1/H_4$ . The final response for the disturbance shown in figure 1(c) may then be obtained from the following equation:

$$\begin{aligned} \frac{\Delta n(s)}{\Delta n_s} = & \frac{1}{H_1} I(s) - \frac{1}{H_1} I(s - H_1) - \frac{1}{H_2} I(s - H_1) \\ & + \frac{1}{H_2} I(s - H_1 - H_2) - \frac{1}{H_3} I(s - H_1 - H_2) + \frac{1}{H_3} I(s - H_1 - H_2 - H_3) \\ & + \frac{1}{H_4} I(s - H_1 - H_2 - H_3) - \frac{1}{H_4} I(s - H_1 - H_2 - H_3 - H_4) \end{aligned} \quad (12)$$

Although equation (12) appears very lengthy, the actual computations are relatively simple since all the integrals for a particular mass parameter have already been determined (fig. 3). The values of each integral multiplied by its appropriate constant can be tabulated in separate columns displaced by its corresponding interval. The addition of the elements in each row of these columns will determine the final response  $\frac{\Delta n(s)}{\Delta n_s}$ .

### Triangular Gust

Since the triangular gust shown in figure 1(d) was used in many calculations, a chart was prepared for this specific shape. The response to this type of disturbance for a range of mass parameters  $\mu_g$  and gradient distances  $H$  was obtained by the method previously described for gust shapes approximated by straight lines. Plotting the maximum values of these responses  $\left(\frac{\Delta n}{\Delta n_s}\right)_{\max}$  as a function of  $H$  with  $\mu_g$  as a parameter gives the chart shown in figure 4. As a matter of interest the values of  $\left(\frac{\Delta n}{\Delta n_s}\right)_{\max}$  are plotted as a function of  $\mu_g$  with the gradient distance  $H$  as the parameter in figure 5. When the mass parameter of the airplane (equation (3)) and the gradient distance  $H$  are known, the value of  $\left(\frac{\Delta n}{\Delta n_s}\right)_{\max}$  is readily obtained directly. Evaluating  $\Delta n_s$  by equation (2) permits the value of  $\Delta n_{\max}$  in a triangular gust to be determined from the acceleration ratio  $\left(\frac{\Delta n}{\Delta n_s}\right)_{\max}$ .

### CONCLUDING REMARKS

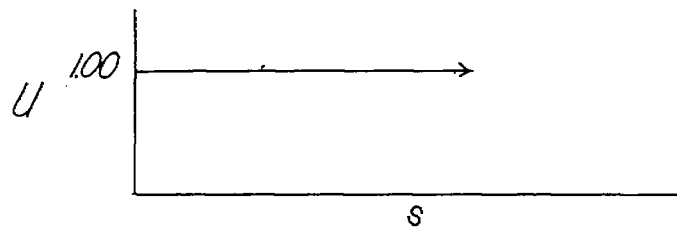
The simplified equation of vertical motion of an airplane has been solved to obtain charts of acceleration ratio for different gust shapes.

The results permit the rapid estimation of maximum acceleration ratios for gusts of arbitrary shape.

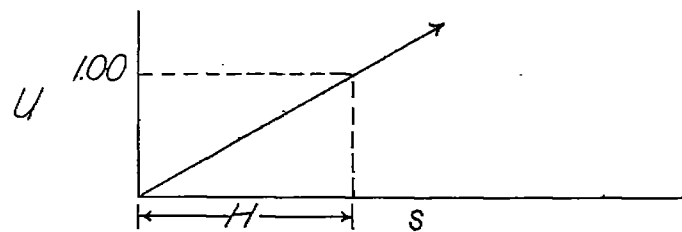
Langley Aeronautical Laboratory  
National Advisory Committee for Aeronautics  
Langley Air Force Base, Va., August 1, 1949.

#### REFERENCES

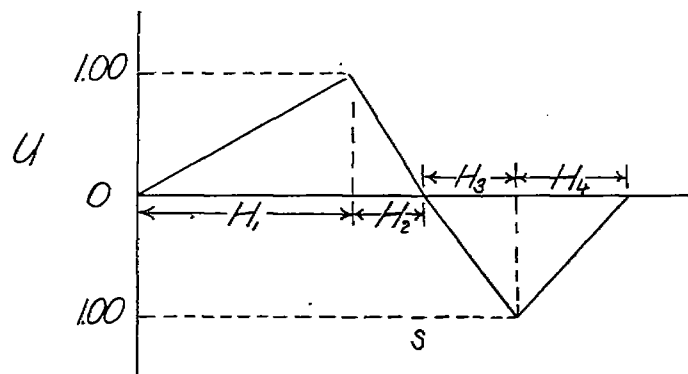
1. Mazelsky, Bernard, and Diederich, Franklin W.: A Method of Determining the Effect of Airplane Stability on the Gust Load Factor. NACA TN 2035, 1950.
2. Jones, Robert T.: The Unsteady Lift of a Wing of Finite Aspect Ratio. NACA Rep. 681, 1940.
3. Von Karman, Theodore, and Biot, Maurice A.: Mathematical Methods in Engineering. First ed., McGraw-Hill Book Co., Inc., 1940, pp. 403-405.
4. Mazelsky, Bernard, and Diederich, Franklin W.: Two Matrix Methods for Calculating Forcing Functions from Known Responses. NACA TN 1965, 1949.



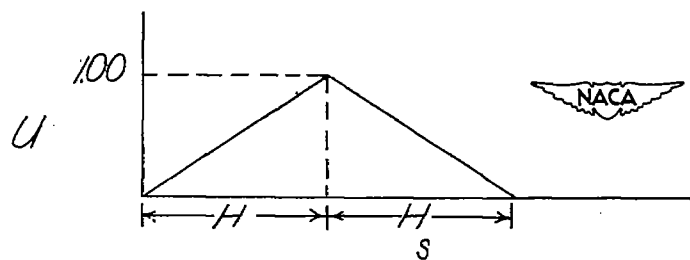
(a) Sharp-edge gust.



(b) Gradient gust.



(c) Arbitrary gust shape approximated by straight lines.



(d) Triangular gust.

Figure 1.- Gust shapes.

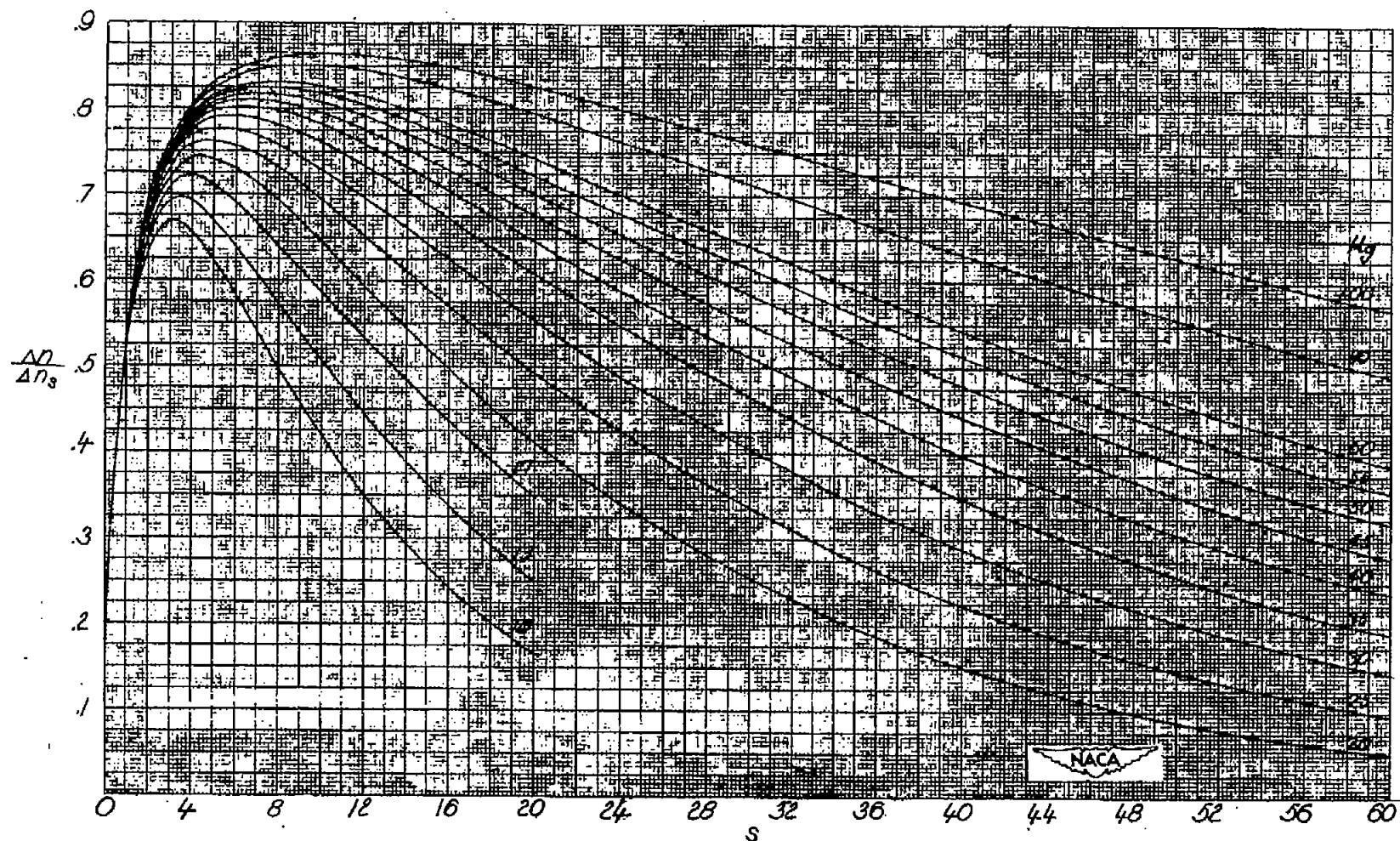


Figure 2.- Acceleration ratio for a wing penetrating a sharp-edge gust for various mass parameters.

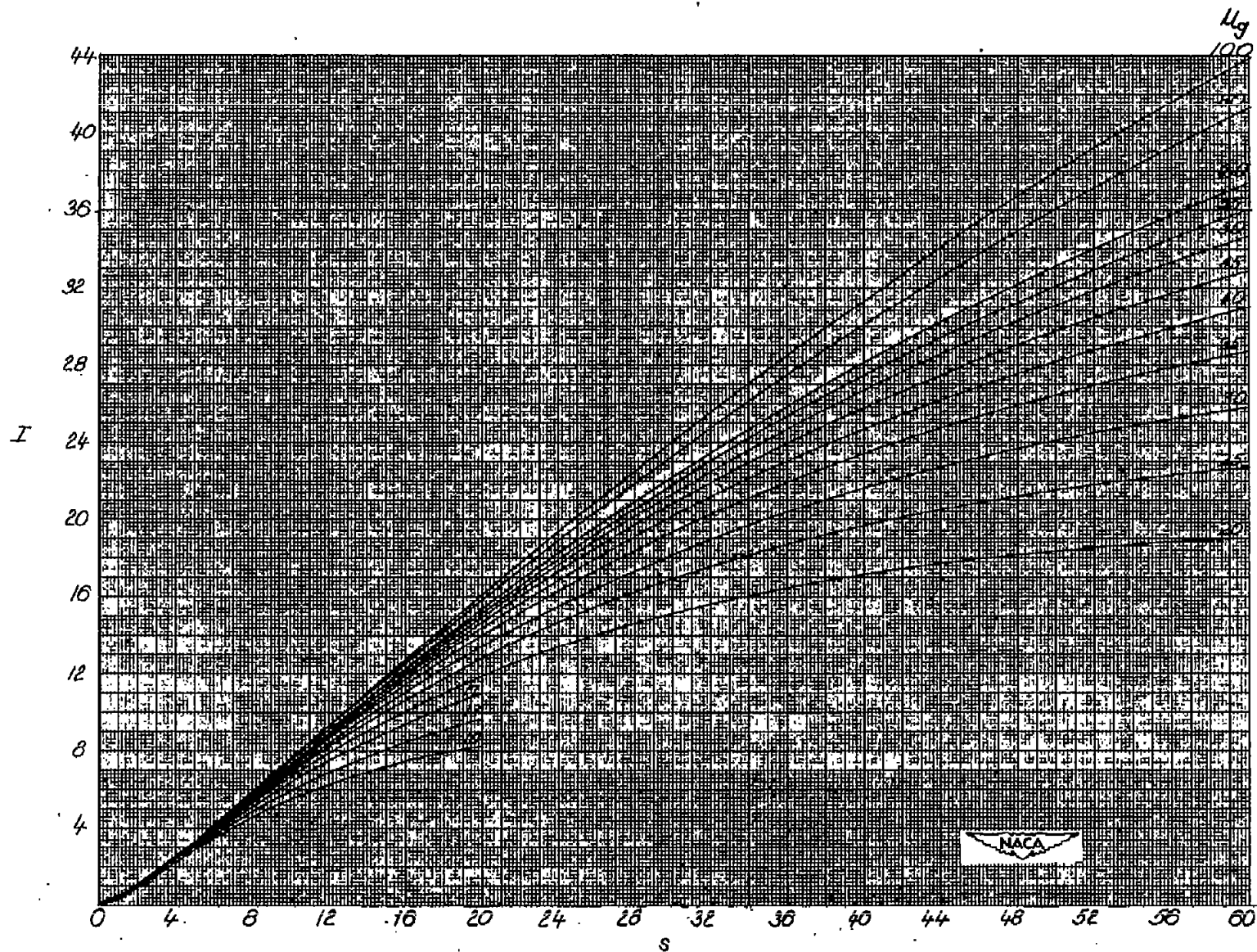


Figure 3.- Integration of acceleration ratio for a wing penetrating a sharp-edge gust for various mass parameters.

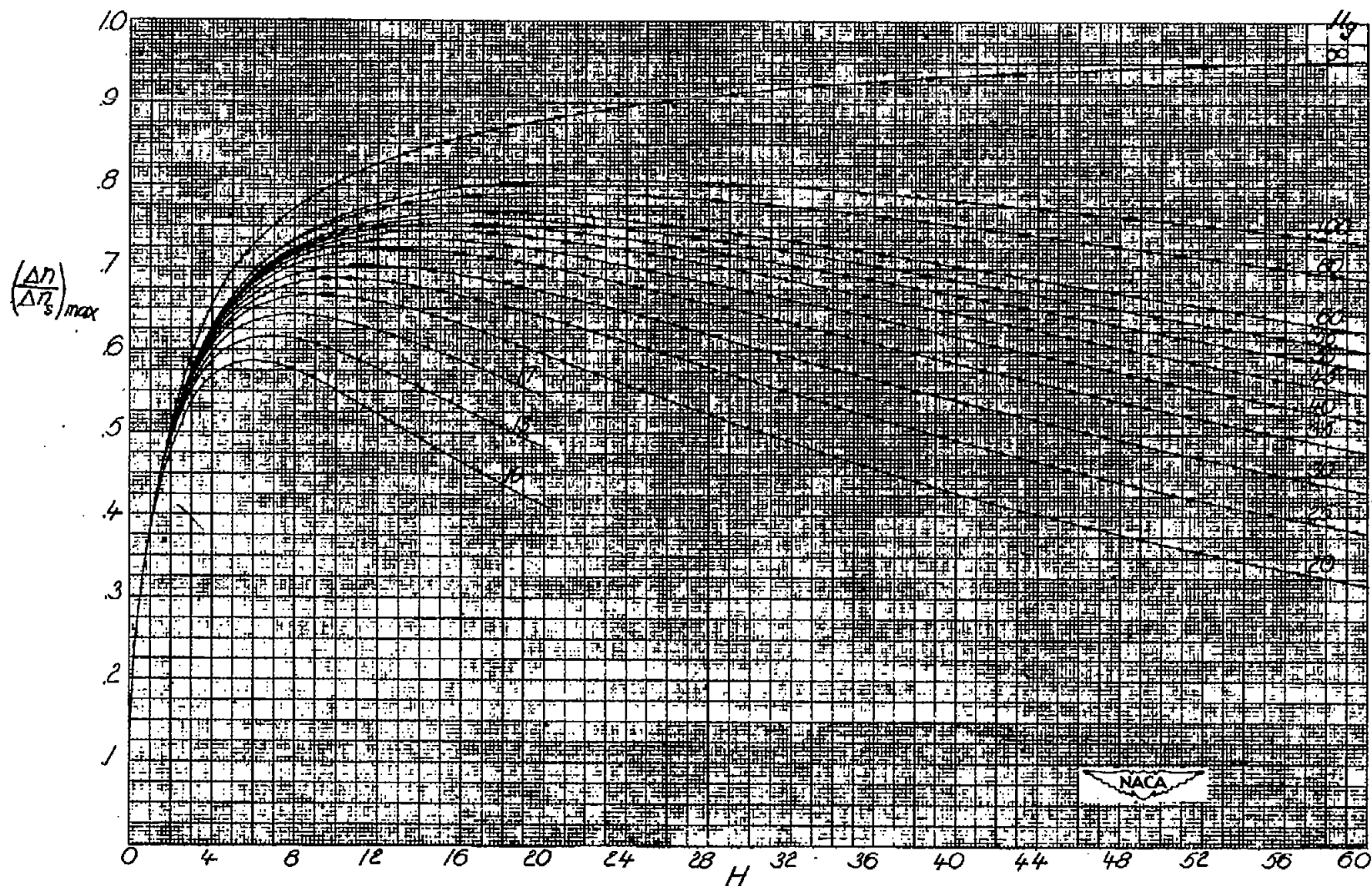


Figure 4.- Maximum acceleration ratio for a triangular gust as a function of gradient distance.

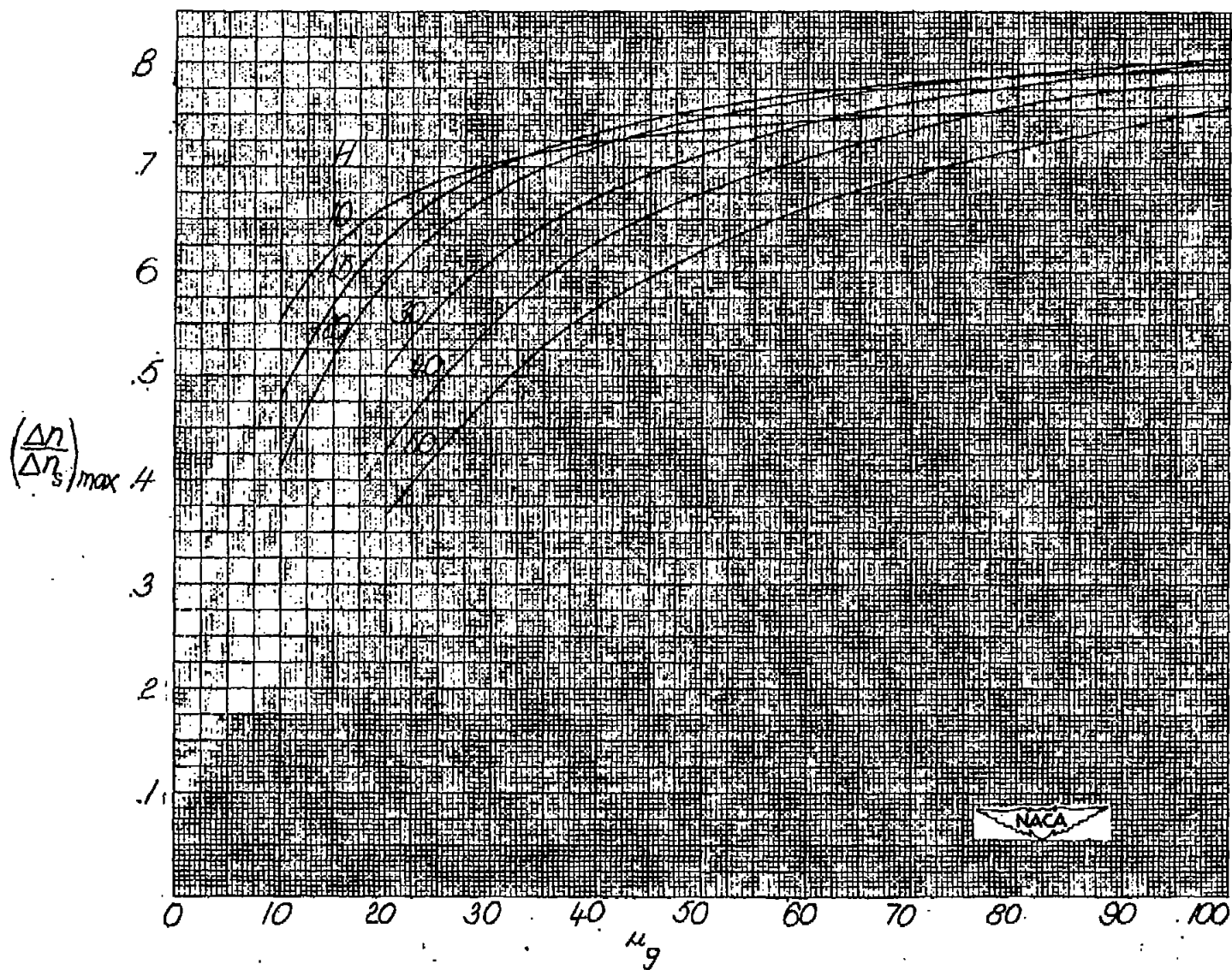


Figure 5.- Maximum acceleration ratio for a triangular gust as a function of mass parameter.